

# A FUZZY ANT COLONY OPTIMIZATION ALGORITHM FOR THE ESTIMATION OF RADIATIVE PROPERTIES IN ONE-DIMENSIONAL HOMOGENEOUS PARTICIPATING MEDIA

**Roberto Pinto Souto, roberto.souto@crs.inpe.br**

Centro Regional Sul/INPE

**Eduardo Fávero Pacheco da Luz, eduardo.luz@lac.inpe.br**

Pós-graduação em Computação Aplicada/INPE

**José Carlos Becceneri, becce@lac.inpe.br**

**Stephan Stephany, stephan@lac.inpe.br**

**Haroldo Fraga de Campos Velho, haroldo@lac.inpe.br**

Laboratório de Computação e Matemática Aplicada/INPE

**Sandra Aparecida Sandri, sandri@iia.csic.es**

Artificial Intelligence Research Institute/IIIA-CSIC

**Antonio José da Silva Neto, ajsneto@iprj.uerj.br**

Instituto Politécnico/UERJ

**Abstract.** *Inverse radiative heat transfer problems have several relevant applications in many different areas such as astronomy, environmental sciences, engineering and medicine. Some outstanding examples are parameter and function estimation for global climate models, hydrologic optics, and computerized tomography. When formulated implicitly, inverse problems are usually written as optimization problems. Several heuristics that mimic nature behavior have been proposed for the solution of optimization problems. In particular some of the most recent algorithms, classified within the field of swarm intelligence, are based on the observation of social insects behavior. In the last decade of the past century the Ant Colony System (ACS) was applied successfully for the solution of combinatorial optimization problems, and more recently it has been proposed for the solution of some specific inverse problems associated to the estimation of real-valued parameters. In the present work is presented a variation of the ACS optimization method, the so called Fuzzy ACS (F-ACS), for the solution of an inverse radiative transfer problem in which we seek to determine the optical thickness, the single scattering albedo and the diffuse reflectivities at the inner side of the boundaries of a one-dimensional participating medium. Here we include a fuzzy component to the path of each agent (ant) in order to improve the performance of the method. As experimental data we consider the intensity of the emerging radiation measured at the boundary surfaces of the medium using only external detectors. The computational implementation of the F-ACS is discussed and results are presented for a few test cases demonstrating the feasibility of the use of the proposed methodology.*

**Keywords:** *inverse problems; radiative transfer; participating media; stochastic methods; computational intelligence*

## 1. INTRODUCTION

Inverse radiative heat transfer problems have several relevant applications in many different areas such as astronomy, environmental sciences, engineering and medicine (Chedin et al., 2003, Craig and Brown, 1986, Hakim and McCormick, 2003, Miesch et al., 2003, Siewert, 2002). Some outstanding examples are parameter and function estimation for global climate models, hydrologic optics, and computerized tomography (Becceneri and Sandri, 2006, Campos Velho et al., 2003a, Campos Velho et al., 2003b, Gao et al., 1998, Hochberg et al., 2003, Zhou et al., 2002).

When formulated implicitly (Silva Neto, 2002), inverse problems are usually written as optimization problems. Several heuristics that mimic natural behaviors have been proposed for the solution of optimization problems. In particular some of the most recent algorithms, classified within the field of swarm intelligence (Bonabeau, Dorigo and Theraulaz, 1999), are based on the observation of social insects behavior.

In the last decade of the past century the Ant Colony System (ACS) was applied successfully for the solution of combinatorial optimization problems (Dorigo, Maniezzo and Colorni, 1996), and more recently it has been proposed for the solution of some specific inverse problems associated to the estimation of real-valued parameters (Becceneri and Zinober, 2001, Souto et al., 2004, Stephany et al., 2009). In most implementations of ACS for graph problems, an ant lays down pheromone only on the edges connecting the nodes in its path. However, to be more realistic, the pheromone should be modeled as an odor exhaling substance and, as such, the closest an ant would be to a trail of pheromone, the stronger should the perceived odor be. To mimic that characteristic, Becceneri and Sandri (2006) proposed the use of ACS with

fuzzy pheromone dispersion, called F-ACS for short. In this approach, an ant is allowed to deposit pheromone not only on the edges in its path, but also on edges close to them. One of the main issues in this approach is thus to define a scheme for the pheromone dispersion that implements the fuzzyfication. One application of F-ACS to the inverse problem was carried out by Carvalho et al. (2008).

In the present work is presented the application of F-ACS for the solution of an inverse radiative transfer problem in order to estimate the optical thickness, the single scattering albedo and the diffuse reflectivities at the inner side of the boundaries of a one-dimensional participating medium. The experimental data is the intensity of the emerging radiation measured at both boundary surfaces of the medium using only external detectors.

## 2. MATHEMATICAL FORMULATION OF THE DIRECT AND INVERSE RADIATIVE TRANSFER PROBLEMS

### 2.1 Direct problem

In Fig. 1 is represented a one-dimensional, gray, homogeneous, isotropically scattering participating medium, of optical thickness  $\tau_0$  whose boundaries reflect diffusely the radiation that comes from the interior of the medium. The boundary surfaces at  $\tau = 0$  and  $\tau = \tau_0$  are subjected to the incidence of radiation originated at external sources with intensities  $A_1$  and  $A_2$ , respectively.

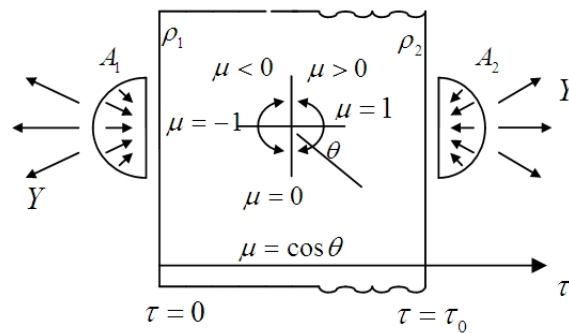


Figure 1. Schematical representation of a one-dimensional participating medium subjected to the incidence of radiation from external sources.  $Y$  represents the intensity of the emergent radiation that may be measured by external detectors.

The mathematical model for the interaction of the radiation with the participating medium is given by the linear version of the Boltzmann equation (Özsisik, 1973),

$$\mu \frac{\partial I(\tau, \mu)}{\partial \tau} + I(\tau, \mu) = \frac{\omega}{2} \int_{-1}^1 I(\tau, \mu') d\mu', \quad 0 < \tau < \tau_0, \quad -1 \leq \mu \leq 1 \quad (1)$$

$$I(0, \mu) = A_1(\mu) + 2\rho_1 \int_0^1 I(0, -\mu') \mu' d\mu', \quad \mu > 0 \quad (2)$$

$$I(\tau_0, -\mu) = A_2(\mu) + 2\rho_2 \int_0^1 I(\tau_0, \mu') \mu' d\mu', \quad \mu < 0 \quad (3)$$

where  $I$  represents the radiation intensity,  $\tau$  is the optical variable,  $\mu$  is the cosine of the polar angle, i.e. the angle formed between the radiation beam and the positive  $\tau$  axis,  $\omega$  is the single scattering albedo, and  $\rho_1$  and  $\rho_2$  are the diffuse reflectivities at the inner part of the boundary surfaces at  $\tau = 0$  and  $\tau = \tau_0$ , respectively. The other symbols have already been defined.

When the geometry, the boundary conditions, and the radiative properties are known, the problem may be solved and the radiation intensity  $I$  determined for the whole spatial and angular domains, i.e.  $0 \leq \tau \leq \tau_0$ , and  $-1 \leq \mu \leq 1$ . This is the so called direct problem.

In order to solve the problem, we use Chandrasekhar's discrete ordinates method (Chandrasekhar, 1960) in which the polar angle domain is discretized as represented in Fig. 2, and the integral term (in-scattering) on the right hand side of Eq. (1) is replaced by a Gaussian quadrature.

We then used a finite-difference approximation for the terms on the left hand side of Eq. (1), and by performing

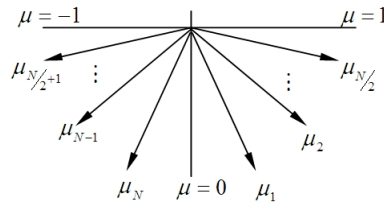


Figure 2. Discretization of the polar angle domain.

forward and backward sweeps, from  $\tau = 0$  to  $\tau = \tau_0$  and from  $\tau = \tau_0$  to  $\tau = 0$ , respectively,  $I(\tau, \mu)$  is determined for all spatial and angular nodes of the discretized computational domain.

### 2.2 Inverse problem

We now consider that the following vector of radiative properties is unknown

$$\vec{Z} = \{\tau_0, \omega, \rho_1, \rho_2\}^T \tag{4}$$

but experimental data on the intensity of the radiation that leaves the medium is available, i.e.  $Y_i, i = 1, 2, \dots, N$ . As schematically represented in Fig. 3, half of the data is acquired at the boundary  $\tau = 0$ , and half at  $\tau = \tau_0$ , using only external detectors.

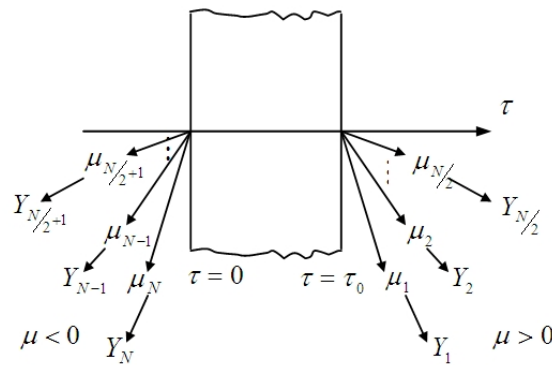


Figure 3. Schematic representation of the experimental data  $Y_i, i = 1, 2, \dots, N/2$  acquired at  $\tau = \tau_0$ , and  $Y_i, i = N/2 + 1, N/2 + 2, \dots, N$  acquired at  $\tau = 0$ .

From the experimental data available, we then try to obtain estimates for the unknown radiative properties. This is the inverse radiative transfer problem we want to solve.

As the number of experimental data,  $N$ , is usually larger than the number of unknowns, we may formulate the inverse problem as a finite dimensional optimization problem in which we seek to minimize the cost function (also known as objective function) given by the summation of the squared residues between calculated and measured values of the radiation intensity,

$$Q(\vec{Z}) = \sum_{i=1}^N [I_{calc_i}(\tau_0, \omega, \rho_1, \rho_2) - Y_i]^2 \tag{5}$$

This inverse problem will be solved by the F-ACS.

### 3. THE ANT COLONY SYSTEM

The Ant Colony System (ACS) is a method that employs a metaheuristic based on the collective behavior of ants choosing a path between the nest and the food source (Dorigo, Maniezzo and Colomi, 1996). Each ant marks its path with an amount of pheromone, and the marked path is further employed by other ants as a reference. As an example of this, the sequence in Fig. 4 shows how ants, trying to go from point  $A$  to point  $E$  (Fig. (4a)), behave when an obstacle is put in the middle of the original path, blocking the flow of the ants between points  $B$  and  $D$  (Fig. (4b)). Two new paths are

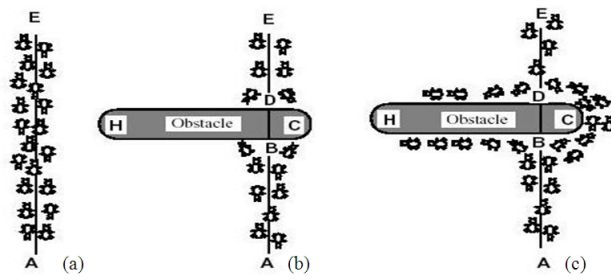


Figure 4. Paths followed by a group of ants from the nest ( $A$ ) to the food source ( $E$ ), (Dorigo, Maniezzo and Colomi, 1996). (a) free path, (b) blockage caused by an obstacle, and (c) search for alternative paths with a concentration of ants on the shortest one ( $ABCDE$ ).

then possible, either going to the left of the obstacle (point  $H$ ) or to the right (point  $C$ ). The shortest path causes a greater amount of pheromone to be deposited by the preceding ants and thus more and more ants choose this path (Fig. (4c)).

The behavior of the ants represented schematically in Fig. 4 is then used for the formulation and solution of an optimization problem.

In the ACS optimization method, several generations of ants are produced. For each generation, a fixed amount of ants ( $na$ ) is evaluated. Each ant is associated to a feasible path that represents a candidate solution, being composed of a particular set of edges of the graph that contains all possible solutions. Figure 5 represents the discretization of the feasible range for each unknown. Here we consider that the range for each of the  $ns$  unknowns,  $\tau_0$ ,  $\omega$ ,  $\rho_1$  and  $\rho_2$ , is discretized in  $np = 128$  values. Each unknown is then depicted as a range of discretized values and is considered a node of the problem. Each ant consists on a set of edges that links a set of nodes (one for each unknown). Each edge is defined by a pair of randomly chosen values of the corresponding unknowns. Figure 5 also shows three ants, being each one composed by its own set of edges. Choosing the unknowns on a probabilistic basis generates each ant. This approach was successfully used for the Traveling Salesman Problem (TSP) and other graph like problems (Becceneri and Zinober, 2001). The best ant of each generation is then chosen and it is allowed to mark with pheromone its path. This will influence the creation of ants in further generations. The pheromone put by the ants decays according to an evaporation rate denoted by  $\phi_{decay}$ . Finally, at the end of all generations, the best solution is assumed to be achieved. A solution (ant) is generated by linking the  $ns$  nodes by  $(ns - 1)$  edges. In order to connect each pair of nodes,  $np$  discrete values can be chosen. This approach was developed in order to deal with real valued unknowns. In our inverse radiative transfer problem  $ns$  corresponds to the total number of unknowns, i. e.  $ns = 4$ , as shown in Eq. (4) and in Fig. 5. All possible edges are represented by an array  $[i, j]$  with  $i = 1, 2, \dots, ns$  and  $j = 1, 2, \dots, np$ , being therefore  $ns \times np$  possible edges available.

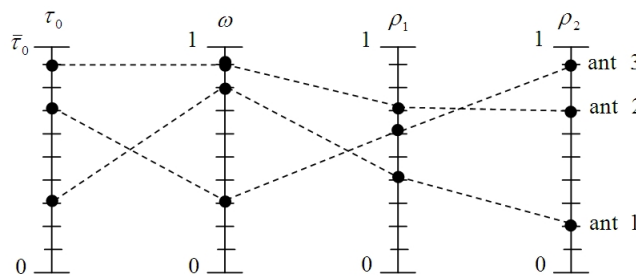


Figure 5. Schematical representation of the random generation of three ants.

At the beginning of the algorithm, generation  $k = 0$ , all nodes of the array  $[i, j]$  are assigned with the following concentration of pheromone  $\phi_{ij}^{k=0} = \phi_0$ . The amount  $\phi_0$  is calculated with a greedy heuristics, as suggested in Bonabeau, Dorigo and Theraulaz (1999), using an evaluation of the objective function  $Q(\vec{Z})$  given by Eq. (5),

$$\phi_0 = \frac{1}{ns \times Q(\vec{Z}^*)} \quad (6)$$

As in the inverse problems we are not able to determine a priori a greedy heuristics, we decided to arbitrarily choose  $\vec{Z}^* = \{\tau_0^*, \omega^*, \rho_1^*, \rho_2^*\}^T = \{1, 1, 1, 1\}^T$  in order to evaluate  $Q(\vec{Z}^*)$  to be used in Eq. (6).

The best ant in a given generation is allowed to mark its path, i.e. its set of edges, with the maximum amount of pheromone, and this will have an influence on the choice of the ants in the following generation. Therefore, for the next generations,  $k = 1, 2, \dots$ , the amount of pheromone for all nodes is given by

$$\phi_{ij}^k = (1 - \phi_{decay}) \phi_{ij}^{k-1} + \delta_{ij,best}^{k-1} \phi_0 \quad (7)$$

where  $\delta_{ij,best}^{k-1}$  is the Kronecker delta associated with the best ant in generation  $k - 1$ , i.e. the one who yields the lowest value for the objective function at the preceding generation ( $k - 1$ ).

The probability of a given edge  $[i, j]$  to be chosen at generation  $k$  is given by (Bonabeau, Dorigo and Theraulaz, 1999, Dorigo, Maniezzo and Colorni, 1996)

$$P_{ij}^k = \frac{[\phi]_{ij}^k \alpha [\eta_{ij}]^\beta}{\sum_{l=1}^{np} \{ [\phi]_{il}^k \alpha [\eta_{il}]^\beta \}} \quad (8)$$

where  $\eta_{ij}$  is the visibility/cost of each edge, a concept that arises from the TSP, where the cost is the inverse of the distance of a particular edge.

In Eq. (8) we assume that all edges are possible for any ant. The parameters  $\alpha$  and  $\beta$  are weights used to establish a tradeoff between the influence of the pheromone and the visibility in the probability of choosing a given edge.

There is an additional scheme for the choice of an edge for a new ant. According to roulette, a random number in the range  $[0, 1]$  is generated for the new ant and it is compared with a parameter  $q_0$  chosen for the problem. If the random number is greater than this parameter, the path is taken according to  $P_{ij}$  in Eq. (8). If not, the most marked edge is assigned.

In our inverse radiative transfer problem each ant corresponds to a candidate solution. The ranges of the unknowns are given by  $0 \leq \omega, \rho_1, \rho_2 \leq 1$  according to the physics of the problem, and  $0 \leq \tau_0 \leq \bar{\tau}_0$  (this unknown is mathematically unbounded in the upper limit). Nonetheless, in practical applications related to the solution of real inverse problems, we may consider an artificial upper bound. Here we have considered  $\bar{\tau}_0 = 1$ . Note that for the calculation of  $\phi_0$  in Eq. (6) we have used the upper bounds for all the unknowns in  $\vec{Z}^*$  in order to determine  $Q(\vec{Z}^*)$ .

We do not assume any stopping criteria for the iterations considering inversions from noiseless or noisy data. A fixed number of iterations is considered (according to the test case, 25, 50 200, 800 or 1600 iterations) and the chosen solution is chosen among the best ants of all the iterations, that is not necessarily the best ant of the last iteration.

In the present work we have not included any visibility information,  $\eta_{ij}$ . For instance, Stephany et al. (2009) considered the smoothness of the path as the visibility information for the estimation of the diffusion coefficient in a crystal growth inverse problem. The smoothness was then measured using Tikhonov's regularization terms (Tikhonov and Arsenin, 1977).

The feasibility of including visibility information for the inverse radiative transfer problem will be investigated in future works. In such case, we will consider also the use of a regularization term in Eq. (5).

### 3.1 ACS with pheromone dispersion

In the Ant Colony System with fuzzy pheromone dispersion (F-ACS) approach, the best ant lays down a given amount of pheromone on the edges that compose its path, but also lays down smaller quantities of pheromone on the adjacent edges. Figure 6 illustrates this pheromone dispersion: the bold marked edge that corresponds to the best solution is marked with an amount  $\tau_0$  of pheromone, whereas its adjacent edges are marked with lesser amounts of pheromone (40% and 10% of  $\tau_0$  respectively). In the present dispersion scheme, adjacent edges are only considered if they not exceed the limiting ranges of the properties to be estimated.

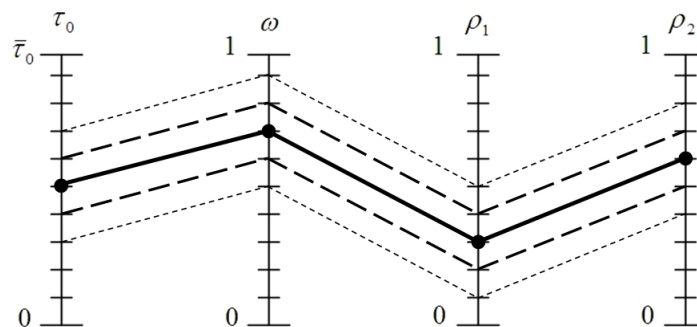


Figure 6. Example of pheromone dispersion. The continuous line represents the path with full deposition of pheromone ( $\tau_0$ ), the thick and the thin dashed lines represent the paths with 40% and 10% of  $\tau_0$ , respectively.

#### 4. RESULTS AND DISCUSSIONS

As in most of stochastic optimization algorithms (and also deterministic algorithms), the quality of the solution obtained is related to the proper choice and fine tuning of the control parameters. For the F-ACS implementation performed in the present section we have considered:  $\phi_{decay} = 0.30$  for the pheromone decay rate and  $q_0 = 0.0$  for the parameter related to the choice of a new edge; this value implies that edges are chosen according to Eq. (8). In this equation, since visibility was not taken into account, the control parameters were taken as  $\alpha = 1$  and  $\beta = 0$ .

We are interested in the estimation of the four unknown radiative properties given in Eq. (4). The range for each of the unknowns, already defined in Section 3 as being  $0 \leq \omega, \rho_1, \rho_2, \tau_0 \leq 1$ , is discretized into 100 values. Therefore, as explained in the previous section,  $ns = 4$  and  $np = 100$ . A total of 50 generations ( $nit = 50$ ) are performed for each run of the F-ACS minimizer. At each iteration we consider a total number of  $na = 16$  ants.

In the case of noiseless data, we generated synthetic experimental data corresponding to the emergent radiation intensities by using the direct model with the exact values of the radiative properties. As real experimental noisy data was not available, we corrupted the noiseless data with Gaussian noise using a standard NAG (Numerical Algorithms Group) routine. In all test cases we have considered noiseless data as well as data corrupted with 2% and 5% gaussian noise.

In order to evaluate the performance of the F-ACS minimizer we chose a relatively difficult test case with

$$\vec{Z}_{exact} = \{\tau_0, \omega, \rho_1, \rho_2\}^T = \{1.00, 0.50, 0.10, 0.95\} \quad (9)$$

The incident radiation was taken as  $A_1 = 1.0$  and  $A_2 = 0.0$  in Eqs. (2) and (3), respectively. The main difficulty for the solution of the inverse radiative transfer problem considered in this work is related to the estimation of  $\rho_1$  since its effect will be sensed by the external detectors only after the radiation goes into the medium at  $\tau = 0$ , is reflected at  $\tau = \tau_0$  and is then both transmitted and reflected at  $\tau = 0$ . This difficulty is confirmed by the sensitivity analysis related to this particular unknown.

For each set of experimental data (noiseless data, and 2% and 5% error noisy data) 10 different runs were performed, using different seeds for the random generation of the ants.

In the following tables are presented the best, worst and average (for the 10 runs) estimated values for the radiative properties. From the second to the fifth columns are shown the exact and estimated values for  $\tau_0, \omega, \rho_1$  and  $\rho_2$ , respectively. In the sixth column are given the values of the cost function,  $Q(\vec{Z})$  defined by Eq. (5), and in the seventh column are presented the values for the square norm between the exact and estimated values for the radiative properties, denominated as *Error* and defined as

$$Error = \sum_{i=1}^4 (Z_i^{exact} - Z_i^{estimated})^2 \quad (10)$$

The F-ACS algorithm is not completely random, since it is somewhat controlled by the probability of generating the ants in a generation according to the amount of pheromone in the previous generation. This is strongly influenced by the seed used for the generation of random numbers employed in the generation of the ants. The use of the same seed may yield solutions that are equal or similar in different test cases (noiseless data and 2% or 5% noisy data).

Table 1 presents the results obtained previously by the application of canonical ACS for 128 ants with 200 iterations over the inverse problem described in Section 2 (Souto et al., 2005) for noiseless, 2% and 5% noisy data. In the same work (Souto et al., 2005) a hybridization of ACS with the Levenberg-Marquardt (LM) method was conducted by using a brief execution of ACS (16 ants and 25 iterations) to generate an initial guess to the LM method, leading to excellent mean results, not shown here.

Table 2 shows inversions performed from noiseless data with the 16-ant F-ACS, considering 20, 50, 200, 800 and 1600 iterations. The results of the F-ACS with 200 iterations (Table 2) are similar than those of the former work (Table 1), but at a lower computational cost, since only 1/8 of the ants are evaluated (16 instead of 128). However, in this case, the F-ACS achieved the exact solution for two seeds, beating those results obtained with the ACS-LM hybridization. It can be also observed in both tables that the noise affects the quality of the inversions, but that the F-ACS is able to reach better solutions using noisy data for a higher number of iterations, and at an equivalent processing cost (128 ants/200 iterations versus 16 ants/1600 iterations). Finally, Table 3 presents the inversions obtained with the 16-ant F-ACS and 50 iterations for noiseless and for noiseless, 2% and 5% noisy data. Solutions with acceptable quality were obtained at a very low computational cost (only 800 evaluations). We observed that, in comparison to the canonical ACS, the F-ACS is slightly slower to converge, but it is possibly more robust, since the quality of its solutions improves steadily with the increase of the number of iterations. A more extensive study will be conducted in order to evaluate the use of the mode obtained by the execution of several seeds. This approach seems promising, since the discretization of the search space is a prerequisite for the application of ACS in real valued problems.

Table 1. Results obtained by the canonical ACS for 128 ants with 200 iterations.

|                         | $\tau_0$ | $\omega$ | $\rho_1$ | $\rho_2$ | $Q(\vec{Z})$ , Eq. (5) | Error, Eq. (10) |
|-------------------------|----------|----------|----------|----------|------------------------|-----------------|
| <b>Noiseless data</b>   |          |          |          |          |                        |                 |
| best (seed 01)          | 0.99     | 0.50     | 0.13     | 0.95     | 7.78E-06               | 1.21E-03        |
| worst (seed 75)         | 0.95     | 0.55     | 0.28     | 0.96     | 6.06E-05               | 4.11E-02        |
| average                 | 0.98     | 0.52     | 0.19     | 0.95     | 2.57E-05               | 9.62E-03        |
| <b>2% noisy data</b>    |          |          |          |          |                        |                 |
| best (seed 49)          | 0.96     | 0.50     | 0.13     | 0.95     | 1.05E-04               | 2.50E-03        |
| worst (seed 01)         | 0.92     | 0.53     | 0.25     | 0.95     | 1.50E-04               | 2.98E-02        |
| average                 | 0.94     | 0.52     | 0.21     | 0.95     | 1.26E-04               | 1.66E-02        |
| <b>5% noisy data</b>    |          |          |          |          |                        |                 |
| best (seed 01)          | 0.90     | 0.48     | 0.13     | 0.95     | 6.40E-04               | 1.13E-03        |
| worst (seeds 37 and 75) | 0.84     | 0.53     | 0.32     | 0.96     | 6.88E-04               | 7.50E-02        |
| average                 | 0.87     | 0.52     | 0.25     | 0.96     | 6.63E-04               | 3.94E-02        |
| Exact                   | 1.00     | 0.50     | 0.10     | 0.95     |                        |                 |

Table 2. Results obtained by F-ACS for 16 ants over noiseless data.

|                            | $\tau_0$ | $\omega$ | $\rho_1$ | $\rho_2$ | $Q(\vec{Z})$ , Eq. (5) | Error, Eq. (10) |
|----------------------------|----------|----------|----------|----------|------------------------|-----------------|
| <b>25 iterations</b>       |          |          |          |          |                        |                 |
| best (seed 01)             | 0.99     | 0.47     | 0.02     | 0.95     | 6.15E-05               | 7.40E-03        |
| worst (seed 49)            | 0.76     | 0.42     | 0.19     | 0.97     | 6.21E-03               | 7.25E-02        |
| average                    | 0.86     | 0.52     | 0.25     | 0.96     | 1.62E-03               | 4.21E-02        |
| <b>50 iterations</b>       |          |          |          |          |                        |                 |
| best (seed 21)             | 0.98     | 0.51     | 0.15     | 0.95     | 2.36E-05               | 3.00E-03        |
| worst (seed 49)            | 0.87     | 0.49     | 0.20     | 0.95     | 1.01E-03               | 2.70E-02        |
| average                    | 0.94     | 0.55     | 0.25     | 0.96     | 2.89E-04               | 2.70E-02        |
| <b>200 iterations</b>      |          |          |          |          |                        |                 |
| best (seeds 01 and 55)     | 1.00     | 0.50     | 0.10     | 0.95     | 0.0                    | 0.0             |
| worst (seed 97)            | 0.93     | 0.68     | 0.56     | 0.97     | 2.29E-04               | 2.49E-01        |
| average                    | 0.98     | 0.55     | 0.23     | 0.96     | 6.20E-05               | 1.93E-02        |
| <b>800 iterations</b>      |          |          |          |          |                        |                 |
| best (seeds 01, 11 and 55) | 1.00     | 0.50     | 0.10     | 0.95     | 0.0                    | 0.0             |
| worst (seed 63)            | 0.94     | 0.64     | 0.49     | 0.97     | 2.34E-04               | 1.76E-01        |
| average                    | 0.98     | 0.53     | 0.19     | 0.95     | 4.23E-05               | 9.03E-03        |
| <b>1600 iterations</b>     |          |          |          |          |                        |                 |
| best (seeds 01, 55 and 89) | 1.00     | 0.50     | 0.10     | 0.95     | 0.0                    | 0.0             |
| worst (seed 75)            | 0.97     | 0.55     | 0.26     | 0.95     | 9.43E-05               | 2.90E-02        |
| average                    | 0.99     | 0.52     | 0.16     | 0.95     | 3.17E-05               | 3.78E-03        |
| Exact                      | 1.00     | 0.50     | 0.10     | 0.95     |                        |                 |

Table 3. Results obtained by F-ACS for 16 ant with 50 iterations.

|                       | $\tau_0$ | $\omega$ | $\rho_1$ | $\rho_2$ | $Q(\vec{Z})$ , Eq. (5) | Error, Eq. (10) |
|-----------------------|----------|----------|----------|----------|------------------------|-----------------|
| <b>Noiseless data</b> |          |          |          |          |                        |                 |
| best (seed 21)        | 0.98     | 0.51     | 0.15     | 0.95     | 2.36E-05               | 3.00E-03        |
| worst (seed 49)       | 0.87     | 0.49     | 0.20     | 0.95     | 1.01E-03               | 2.70E-02        |
| average               | 0.94     | 0.55     | 0.25     | 0.96     | 2.89E-04               | 2.70E-02        |
| <b>2% noisy data</b>  |          |          |          |          |                        |                 |
| best (seed 55)        | 0.97     | 0.49     | 0.10     | 0.95     | 1.28E-04               | 1.00E-03        |
| worst (seed 49)       | 0.86     | 0.51     | 0.25     | 0.96     | 5.50E-04               | 4.23E-02        |
| average               | 0.92     | 0.54     | 0.24     | 0.96     | 2.66E-04               | 2.90E-02        |
| <b>5% noisy data</b>  |          |          |          |          |                        |                 |
| best (seed 11)        | 0.91     | 0.47     | 0.09     | 0.95     | 6.60E-04               | 9.10E-03        |
| worst (seed 49)       | 0.69     | 0.54     | 0.47     | 0.97     | 2.05E-03               | 2.35E-01        |
| average               | 0.87     | 0.51     | 0.21     | 0.96     | 8.82E-04               | 2.80E-02        |
| Exact                 | 1.00     | 0.50     | 0.10     | 0.95     |                        |                 |

## 5. ACKNOWLEDGEMENTS

E. F. P. Luz, J. C. Becceneri and H. F. Campos Velho acknowledges the financial support provided by CAPES, Coordenação de Aperfeiçoamento de Pessoal de Nível Superior. A. J. Silva Neto acknowledges the financial support provided

by CNPq and FAPERJ, Fundação Carlos Chagas Filho de Amparo à Pesquisa do Estado do Rio de Janeiro. S. Sandri acknowledges support from the European project Agreement Technologies (CONSOLIDER CSD2007-0022), the Spanish projects MULO2 (TIN2007-68005-C04-01/02) and Autonomic Electronic Institutions (TIN-2006-15662-C02-01), the bilateral project CNPq/CSIC: "IA.GIS.EDERA: use of Artificial Intelligence and Geographical Information Systems for endemic diseases risk analysis" (2007BR0053) and from Generalitat de Catalunya under grant 2005-SGR-00093.

## 6. REFERENCES

- Becceneri, J.C. and Sandri, S., 2006, "Function optimization using ant colony systems", Proc. of IPMU'06, Paris.
- Becceneri, J.C. and Zinober, A.S.I., 2001, "Extraction of energy in a nuclear reactor by ants", Proc. of the Brazilian Symposium on Operations Research, Campos do Jordão, Brazil.
- Bonabeau, E., Dorigo, M. and Theraulaz, G., 1999, "Swarm Intelligence: From Natural to Artificial Systems", Oxford University Press, New York, 307 p.
- Campos Velho, H.F., Vilhena, M.T., Retamoso, M.R. and Pazos, R.P., 2003a, "An application of the LTSN method on an inverse problem in hydrologic optics". Prog. Nucl. Energy, Vol. 42, pp. 457-468.
- Campos Velho, H.F., Ramos, F.M., Chalhoub, E.S., Stephany, S., Carvalho, J.C. and Souza, F.L., 2003b, "Inverse problems in space science and technology", Proc. of the 5th International Conference on Industrial and Applied Mathematics, Sidney, Australia.
- Carvalho, A.R., Campos Velho, H.F., Stephany, S., Souto, R.P., Becceneri, J.C. and Sandri, S., 2008, "Fuzzy Ant Colony Optimization for Estimating Chlorophyll Concentration Profile in OffShore Sea Water", Inv. Problems in Science and Engineering, Vol. 16, No. 6, pp. 705-715.
- Chandrasekhar, S., 1960, "Radiative Transfer", Dover Publications, Inc., New York.
- Chedin, A., Serrar, S., Hollingsworth, A., Armante, R. and Scott, N.A., 2003, "Detecting annual and seasonal variations of CO<sub>2</sub>, CO and N<sub>2</sub>O from a multi-year collocated satellite-radiosonde data-set using the new rapid radiance reconstruction (3R-N) model", J. Quant. Spectrosc. Radiat. Transfer, Vol. 77, pp. 285-299.
- Craig, I.J.D. and Brown, J.C., 1986, "Inverse Problems in Astronomy: A Guide to Inversion Strategies for Remotely Sensed Data", Adam Hilger Ltd., Bristol.
- Dorigo, M., Maniezzo, V. and Colormi, A., 1996, "The ant system: optimization by a colony of cooperating agents", IEEE T. on Syst. Man Cy. B, Vol. 26, No. 2, pp. 29-41.
- Gao, F., Niu, H., Zhao, H. and Zhang, H., 1998, "The forward and inverse models in time-resolved optical tomography imaging and their finite-element method solutions", Image Vision Comput., Vol. 16, pp. 703-712.
- Hakim, A.H. and McCormick, N.J., 2003, "Ocean optics estimation for absorption, backscattering, and phase function parameters", Appl. Optics, Vol. 42, pp. 931- 938.
- Hochberg, E.J., Atkinson, M.J. and Andréfouët, S., 2003, "Spectral reflectance of coral reef bottom-types worldwide and implications for coral reef remote sensing", Remote Sens. Environ., Vol. 85, pp. 159-173.
- Miesch, C., Cabot, F., Briottet, X. and Henry, P., 2003, "Assimilation method to derive spectral ground reflectance of desert sites from satellite datasets", Remote Sens. Environ., Vol. 87, pp. 359-370.
- Özisik M.N., 1973, "Radiative Transfer and Interactions with Conduction and Convection", John Wiley, New York.
- Siewert, C.E., 2002, "Inverse solutions to radiative-transfer problems based on the binomial or the Henyey-Greenstein scattering law", J. Quant. Spectrosc. Radiat. Transfer, Vol. 72, pp. 827-835.
- Silva Neto, A.J., 2002, "Explicit and implicit formulations for inverse radiative transfer problems", Proc. of the 5th World Congress on Computational Mechanics, Vienna, Austria.
- Souto, R.P., Campos Velho, H.F., Stephany, S. and Sandri, S., 2004, "Reconstruction of chlorophyll concentration profile in offshore ocean water using ant colony system", Proc. of the First Hybrid Metaheuristics, Valencia, Spain, pp. 19-24.
- Souto, R.P., Stephany, S., Becceneri, J.C., Campos Velho, H.F., Silva Neto, A.J., 2005, "On the use of the ant colony system for radiative properties estimation", Proc. of the 5th International Conference on Inverse Problems in Engineering - Theory and Practice, Vol. 3, Cambridge, England, pp. 1-10.
- Stephany, S., Becceneri, J.C., Souto, R.P., Campos Velho, H.F. and Silva Neto, A.J., 2009, "A Pre-Regularization Scheme for the Reconstruction of a Spatial Dependent Scattering Albedo Using a Hybrid Ant Colony Optimization Implementation", Applied Mathematical Modelling (in press).
- Tikhonov, A.N. and Arsenin, V.S., 1977, "Solutions of Ill-Posed Problems", Winston and Sons, Washington.
- Zhou, H.-C., Hou, Y.-B., Chen, D.-L. and Zheng, C.-G., 2002, "An inverse radiative transfer problem of simultaneously estimating profiles of temperature and radiative parameters from boundary intensity and temperature measurements", J. Quant. Spectrosc. Radiat. Transfer, Vol. 74, pp. 605-620.

## 7. Responsibility notice

The authors are the only responsible for the printed material included in this paper